2021-04-27

Electrical behavior of CNT epoxy composites under in-situ simulated space environments

Earp, Brian; Hubbard, Joel; Tracy, Alexander; Sakoda, Dan; Luhrs, Claudia

Elsevier

Earp, Brian, et al. "Electrical behavior of CNT epoxy composites under in-situ simulated space environments." Composites Part B: Engineering 219 (2021): 108874. http://hdl.handle.net/10945/67436

Composites Part B 219 (2021) 108874

Contents lists available at ScienceDirect

Composites Part B

journal homepage: www.elsevier.com/locate/compositesb

Electrical behavior of CNT epoxy composites under in-situ simulated space environments

Brian Earp [a,b], Joel Hubbard [a], Alexander Tracy [a], Dan Sakoda [c], Claudia Luhrs [a,c,*]

[a] Mechanical and Aerospace Engineering Department, Naval Postgraduate School, Monterey, CA, 93943, USA
[b] Mechanical Engineering Department, United States Naval Academy, Annapolis, MD, 21402-5042, USA
[c] Space Systems Academic Group, Naval Postgraduate School, Monterey, CA, 93943, USA

ARTICLE INFO

Keywords:
CNT Composites
Conductive composites
Nanocomposite
LEO Space environment
Simulated space

ABSTRACT

The properties of CNT composites are known to suffer changes when exposed to space conditions or simulated space environments. A more in-depth understanding of the magnitude of those changes could help improve the design of systems that contain them, produce more accurate predictions of their performance, or even open the possibility of new applications. In this study, the electrical properties of CNT epoxy composites containing low CNT loadings (less than 1%) were measured *in-situ* while the specimens were exposed to diverse simulated space conditions. A thermal vacuum chamber was employed to produce the low pressures and temperatures associated with low earth orbit. A solar simulator was used to replicate solar irradiance. A convection oven was used to determine the effects that could only be attributed to temperature variations. The changes in resistivity exhibited by the composite specimens are reported for each scenario along possible mechanisms that could explain the observed behavior. The microstructural and thermogravimetric characterization of the composites for the diverse loadings is also presented. Resistivity reductions of up to 40% were observed by the simultaneous application of high temperatures and low pressures, while the application of simulated sunlight with the concomitant surge in temperature, showed a maximum decrease of 58%. Outgassing and an increase in the number of charge carriers at the higher temperatures promoted by the simulated sunlight treatment, are believed to be responsible for the recorded reductions in resistivity. A qualitative analysis of the resistivity changes noted when the composites are exposed back to atmospheric conditions is included.

1. Introduction

The properties of carbon nanotube (CNT) composites have been the subject of a very large number of studies and reports. The scientific community has explored many aspects of these enthralling materials, from measuring and modeling their mechanical, optical, thermal, and electrical properties [1–4], to providing a proof of concept for a vast list of applications that could be fulfilled by their use. CNT composites could be employed as structural materials, batteries, sensors, membranes, and antennas, among others [1,2,5–13]. Due to their light weight, one of the thrust areas that is rapidly developing is the use of CNT composites in space structures and systems. Their specific strength [14], fracture toughness [15,16], fatigue resistance [17–20], and potentially favorable coefficient of thermal expansion [21], make them ideal candidates for space components [7,8,10,12]. CNT composites could also be used in charge dissipation systems and to protect against electromagnetic interference (EMI) [7,8,10,11,22].

The property changes that the composite materials suffer after they are exposed to actual or simulated space environments have been the subject of multiple reports. Low earth orbit (LEO) is of particular importance as the region of space where the International Space Station (ISS) and the Hubble space telescope reside [23,24], as well as a growing commercial space economy that in includes the Iridium constellation of 66 satellites [25]. The StarLink proposed constellation of 42,000 satellites [26] and Planet Labs, Inc.'s more than 150 active earth observation satellites [27], are among other future and current systems located in LEO.

Conditions found in space environments that are known to modify CNT materials include high vacuum, thermal cycles, exposure to atomic oxygen (AO), ultraviolet (UV) and other types of electromagnetic radiation, charged particles and debris [28–30]. LEO, in particular, exposes materials to AO and higher populations of debris [31]. Some of the

* Corresponding author. Mechanical and Aerospace Engineering Department, Naval Postgraduate School, Monterey, CA, 93943, USA.
E-mail address: ccluhrs@nps.edu (C. Luhrs).

https://doi.org/10.1016/j.compositesb.2021.108874
Received 15 December 2020; Received in revised form 30 March 2021; Accepted 4 April 2021
Available online 27 April 2021

consequences of exposure include, but are not limited to, surface erosion, fatigue cracking, loss of volatile components, and delamination [30,32]. For applications focused on charge dissipation and EMI, the changes in electrical properties of the CNT composites are of vital importance. However, the number of reports that focus on these property changes due exposure to the space environment are scarce and do not show, to the best of our knowledge, what instantaneous variations could be expected.

The literature regarding CNT exposure to LEO includes reports for both direct and simulated space environments. Hopkins et al. [33] exposed bare CNT yarns to LEO for more than 2 years by placing samples on the exterior of ISS as part of the Materials International Space Station Experiment (MISSE-8). Their observations include chemical changes and yarn erosion in the outer 1% of the yarn but no catastrophic damage. The study found that the electrical resistivity of the samples was increased by 26.1 and 28.5% depending on the specimen's locations in the ISS. Ishikawa et al. [34] reported similar damage to the CNT yarns after being exposed to the space environment surrounding the ISS and also featured ground-based comparison tests. For the ground-based experiments, the most significant changes in the yarn's performance were related to AO exposure and the substantial reduction in material tensile strength. The electrical conductivity was not modified by exposure to UV or electron beam; however, the team did observe a decrease in resistivity, presumably associated to re-deposition of carbon species. In samples exposed to space, AO irradiation caused significant yarn damage with impacting mechanical properties, however, only minor changes were detected in electrical properties of thick yarns. CNT acid-spun yarns were treated under simulated LEO conditions by Kemnitz et al. [35]. Their observations indicate that UVC radiation did not significantly affect mechanical strength or conductivity but enhanced the piezoresistive effect. In contrast, they observed that AO severely degraded mechanical properties, with a 63.9% decrease in the yarn tensile strength and 56.3% decrease in the strain at failure. AO mildly degraded electrical properties, causing the conductivity to decrease by 22.0%. The mechanical and electrical properties of CNT sheets treated under UVC and vacuum, as simulated LEO conditions, by Cobb et al. [36], confirmed that the effects of UVC exposure on the specimens' microstructure were minimal. In sum, it could be concluded that AO has the potential to increase resistivity of bare CNTs by 20–30%, while the absence of AO, is expected to cause only minor modifications or leave the material unaffected.

Once that the CNT are used as fillers in composites, the outlook of how their properties change as result of LEO exposure is quite different. For example, Jiao et al. [37] studied the AO exposure behavior of CNT epoxy composites, finding that CNT bundles tend to collapse and that porous CNT films present higher levels of erosion than dense counterparts. They also report a decrease in the material tensile strength (16.3% reduction) and electrical conductivity (approx. 30% reduction). The adverse effects of diverse environments, including LEO, in CNT/polymer interfaces were also studied by Prusty et al. [38] The behavior of other carbon composites, such as graphite/epoxy, under simulated LEO settings have shown similar results; the work by Han et al. [39] showed considerable damage to the surface of the composites along mass erosion and reduction of tensile strength due not only to AO, but to the synergistic effects of LEO space environment constituents (AO, UV radiation, thermal cycling).

Reports regarding CNT composites includes work aimed to improve the materials resistance to degradation under LEO conditions. For example, Awaja et al. [40] performed simulated LEO treatments in various carbon epoxy composites, including CNT, and determined the effects that using different reinforcements had on the surface degradation mechanisms of the materials. The experimental conditions used included high vacuum, UV radiation and thermal cycling, the latter employing a halogen lamp and AO generated by a radio frequency power source. The main findings relate to samples with fillers presenting higher oxygen levels and less erosion than the bare epoxy resin. No electrical properties were examined. Atar et al. [41] fabricated flexible and electrically conductive polyimide nanocomposite films using CNT sheets. Their study shows that the incorporation of polyhedral oligomeric silsesquioxane monomer increases the durability of the composites exposed to ground-based AO environments without compromising their electrical conductivity.

The present study focused on characterizing the *instantaneous* changes in electrical properties of epoxy composite specimens containing 0.014, 0.2 and 0.75 wt% of CNT while the samples were subjected to the temperatures, pressures and sunlight exposure that will be expected in LEO conditions. Each of the CNT loadings selected present a different order of magnitude resistivity, thus, prompting an independent *in-situ* analysis. The increasing number of systems located in LEO, and our dependence on their functionalities for advanced communications, global internet services, and earth observations, among others [42], make the subject of this manuscript significant since the results presented inform the community of their expected behavior.

2. Experimental methods

2.1. CNT composites fabrication

The composites studied herein were generated using multiwall carbon nanotubes (MWCNT) acquired from Nanocomp Technologies Inc (Huntsman Corporation, Merrimack, NH, USA) and Henkel Loctite Hysol EA9396 Aero Epoxy (Henkel Corporation, Dusseldorf, Germany). A chemical vapor deposition process using Fe as catalyst was employed to generate large CNT sheets. The sheets, presenting electrical conductivities in the order of 3.2×10^4 S/m (resistivity of 3.125×10^{-3} Ohm-cm) [43], were then converted into a pulp using a Hollander Beater and industrial burr mill [44]. The CNT were used as received, as pulp/-bundles of approximately 0.05 mm diameter and 1 mm in length, with individual nanotube diameter of approximately 30 nm and Fe catalyst nanoparticles dispersed throughout the sample.

The epoxy resin used was a two-part system consisting of resin and hardener, in a manufacturer's recommended mixing ratio of 100:30 by weight. The epoxy system employed is known to have a tensile lap shear strength of 27.6 MPa and a tensile strength of 35.2 MPa at 25 °C when cured for 1 h at 66 °C. The viscosity of the epoxy at 25 °C is 700 Poise for Part A, 0.9 Poise for Part B and 35 Poise for their mixture. The electrical resistivity of the base epoxy mixture is reported to be 2.14×10^{15} Ohm-cm [45].

The resin and the proper amount of CNT to generate the loadings of interest (0.014, 0.2 and 0.75 wt% CNT), were mixed using a FlackTek (Landrum, SC, USA) asymmetric speed mixer operating at 1200 rpm in the first 2 min mixing cycle, at 2500 rpm for 1 min and three subsequent 1 min cycles at 3000 rpm. Vacuum was applied in between mixing cycles to remove air pockets and minimize porosity. The application of vacuum in between mixing cycles also served as a cooling period since the mixing cycles cause the specimen's temperature to increase. Once the CNTs were dispersed in the resin, the hardener was added in a single mixing step. While still in a viscous state, the resin-CNT-hardener mixtures were deposited in an electric board that had a prefabricated pattern of 4 conductive traces to later conduct the electrical measurements. The samples were cured at 66 °C for 1 h using a Binder convection oven (Binder GmbH, Tuttlingen, Germany).

2.2. Simulated space environments

The CNT epoxy composites were exposed to three different environments while their electrical resistivity was measured: a) Tenney thermal vacuum (TVAC) chamber, b) solar simulator and c) convection oven. The first experiment, conducted in the TVAC chamber, was meant to provide similar pressure and temperature conditions to the ones encountered in LEO. The solar simulator was used to mimic the exposure of the specimens to sunlight; thus, the samples electrical properties were

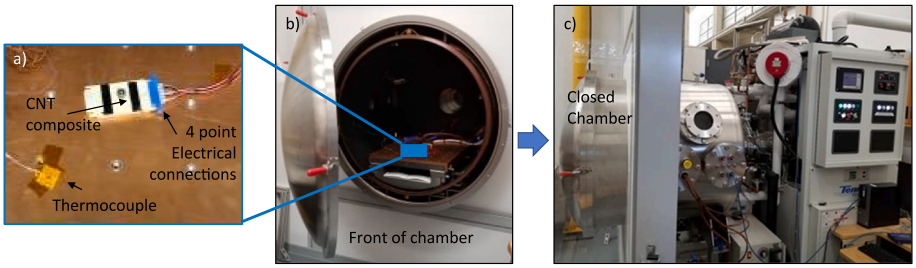

Fig. 1. Tenney environmental chamber setup. a) CNT composite electric board attached to the cables that were used to collect the sample's resistivity data and thermocouple used to verify the platen's temperature. b) Front of the chamber and sample placement. c) Side view of chamber including electronics box used as interface.

measured as a function of irradiance and the temperature increase associated with it. The third set of experiments were conducted inside a convection oven as an attempt to understand the isolated effects of temperature on the composite's resistivity without the influence of pressure or light featured in the other two sets of experiments.

2.2.1. Tenney thermal vacuum TVAC chamber

A TVAC chamber Model 3.5D3-LN2-VTV-G (Tenney Environmental, New Columbia, PA, USA) was employed to subject the CNT composites to pressures and temperatures close to those normally encountered by space systems in LEO. The TVAC system consisted of a stainless-steel vessel operating under high vacuum, with pressures down to 1×10^{-7} Torr [1.3×10^{-5} Pa]. Liquid nitrogen was employed to allow the samples to be cooled, thus, enabling experiments to be carried out in temperatures from −60 °C to +150 °C. Connector pass-through cables were used to collect electrical resistivity data, as shown in Fig. 1. Each of the CNT composites studied (0.014, 0.2 and 0.75 wt% CNT) were tested independently. Two of the loadings were measured twice to verify the run-to-run variation. Resistivity data for multiple temperature points was collected using currents from 5 to 500 μA. For reference and comparison, the pressures encountered at diverse elevations are included in Table 1 below [46].

2.2.2. Solar simulator exposure

An OAI TriSOL 300 mm class AAA solar simulator (Optical Associates Inc., Milpitas, CA, USA) was employed to produce similar conditions than the ones encountered by direct sunlight exposure. Solar simulation light sources of the type employed produce an intense, uniform, collimated beam of broad band energy. The instrument uses a xenon arc lamp to produce the radiation, which is collected by a reflector and directed to an aluminum mirror. The beam then converges onto the optical integrator and the exit beam diverges through the open shutter to the second mirror, where it is reflected through the collimating lens onto the exposure plane. The xenon lamp provides standard sunlight simulation from UV to infrared (IR) in accordance to ASTM E927-5 and ASTM E490. Fig. 2 presents the irradiance graph taken for the instrument covering wavelengths from 330 to 1800 nm; the measurement was performed at 1000 W/m^2 at 25 °C with a lamp current of 82 A. The spectral irradiance wavelength distribution for air mass at global spectrum and zero atmosphere, (AM1.5G and AM0, respectively) are also plotted for reference.

An OAI 306 UV Power meter (Optical Associates Inc. Milpitas, CA, USA) was used to determine irradiance in mW/cm^2 received by the composite specimens for the duration of every experiment. These values are plotted on the secondary axis in the results section (Fig. 8).

Fig. 3 shows the physical arrangement of the samples for the test. Fig. 3a illustrates the placement of the sample in the central region of the simulator exposure plane. It is worth noting that 2 strips of composite are exposed while only one has been soldered to the set of 4 cables for the 4-point resistivity measurements. The source meter was placed at a separate table, its description is included in Section 2.4. Two T-type thermocouples (Omega Engineering, Inc. Norwalk, Connecticut, USA) were employed to measure temperature, one placed on top of the composite and one in direct contact with the high-performance laminar flow isolator that served as substrate. The power meter was located within an inch of the composite's electric board (see Fig. 3b). Fig. 3c shows the simulator during operation, with an open shutter.

2.2.3. Convection oven

The electrical properties of the CNT specimens were also measured inside a convection oven under two different conditions in order to replicate the temperature range and heating rates experienced by the TVAC and solar simulator datasets. For the TVAC comparison, oven temperatures varied from 25 to 150 °C in 10 °C intervals with dwell stabilizing periods in between each step increase. To compare with the solar simulator data, heating in the oven took place from 25 to 90 °C, using a continuous temperature increase until the sample reached the maximum temperature. The same Binder convection oven (Binder GmbH, Tuttlingen, Germany) used for curing the specimens was employed to collect resistivity data as the sample was heated. Fig. 4 shows the sample placement and the experimental setup.

2.3. Materials thermal and microstructural characterization

The cured CNT epoxy samples were analyzed in a Simultaneous Thermal Analyzer (STA) 449 Jupiter F1 (Netzsch GmbH & Co. Holding KG, (Selb, Germany) to determine if the specimens suffered changes in mass as the temperature increased. The data was collected from room temperature to 150 °C with a heating rate of 1°/min under ultra-high purity Argon atmosphere (Ar-UHP) flowing at 100 ml/min.

A Zeiss Neon 40 (Zeiss, Oberkochen, Germany) Dual Beam Scanning Electron Microscope (SEM) operating between 1 and 20 KV was used to determine the microstructural features of the CNT bundles and the distribution of the same along the Fe catalyst in the epoxy resin. A Nikon

Table 1
Altitude pressure conversion table from Ref. [46].

Altitude										
(Feet)	Sea	1000	5000	50,000	100,000	200,000	300,000	500,000	600,000	700,000
(km)	Level	0.3	1.5	15.2	30.5	61.0	91.4	152.4	182.9	213.4
Pressure										
(Torr)	760	733.0	632.5	87.38	8.28	0.169	7.99E-4	1.35E-5	1.76E-6	9.02E-7
(Pa)	1.0E5	9.8E4	8.4E4	1.2E4	1.1E3	2.3E1	1.1E-1	1.8E-3	2.3E-4	1.2E-4

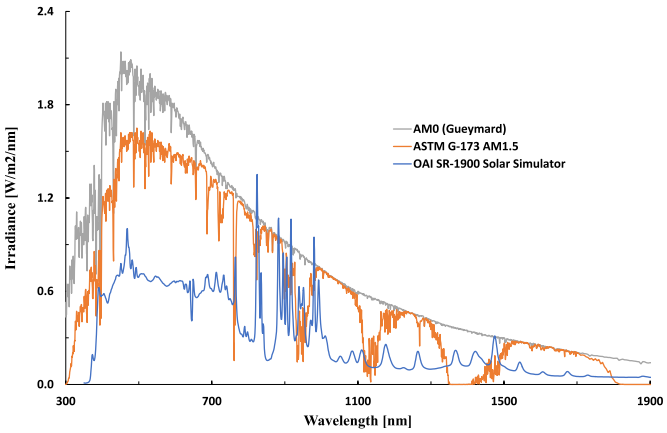

Fig. 2. Measured irradiance for the solar simulator instrument employed in the study with irradiances AM0 and AM1.5 shown for comparison. Modified from source: [47–49].

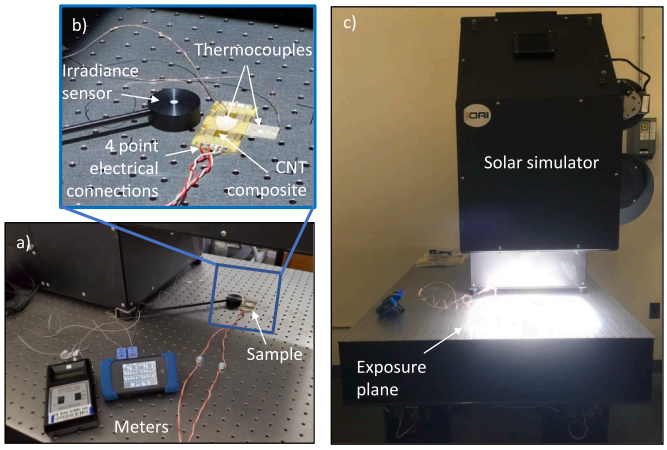

Fig. 3. Solar simulator setup that was employed to simultaneously collect temperature, irradiance and resistivity data. a) Sample placement, b) Meters employed, and c) Image of the exposure plane and view of instrument while shutter is open.

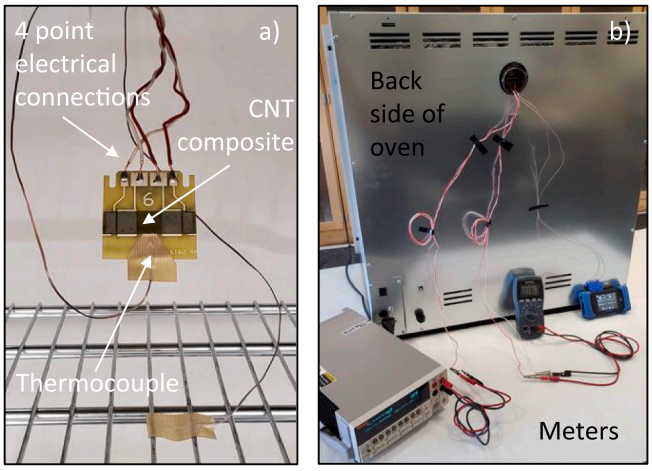

Fig. 4. a) CNT composite board location inside oven and b) Meters and cables employed to conduct 4-point resistivity measurement and corroborate temperature at the board.

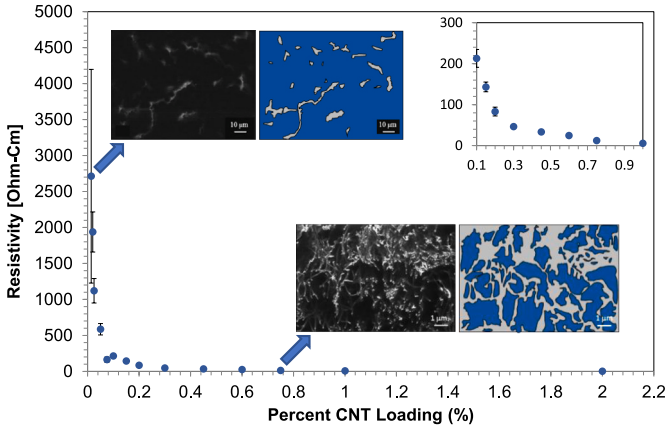

Fig. 5. Epoxy - CNT composite resistivity as a function of CNT loading in wt%. SEM micrographs taken from samples containing different CNT loadings along the schematic representation of the conductive networks that each loading form. Grey regions represent areas where CNT are concentrated, while blue regions constitute the non-conductive zones devoid of CNT. (For interpretation of the references to colour in this figure legend, the reader is referred to the Web version of this article.)

Epiphot 200 reflective optical microscope (Nikon, Tokyo, Japan) was employed to observe the surface porosity of the cured composite samples.

2.4. Electrical measurements

The four-point circuit boards were analyzed using a 2400 Keithley Source Meter (Tektronix, Inc., Beaverton, OR, USA) as the current source and a digital multi-meter to measure the voltage drop across each sample for various applied currents. Using sample thickness, the resistivity of each sample was calculated. For the data reported herein we focused on the resistivity that resulted from the application of 400 μA. In order to determine if the electrical properties effects observed in the samples were permanent or what changes could be expected when the specimens get exposed again to atmospheric conditions, their resistivity was measured immediately after each test, after one day and after multiple days from the time when the original experiment was conducted.

3. Results

3.1. Electrical and microstructural analysis of CNT and CNT composites under atmospheric conditions

In order to understand the significance of the changes in the electrical data observed under simulated LEO conditions for each of the CNT loadings studied, it is indispensable to first describe their microstructures at the nanometer level and the relationship of those with their electrical conductivity at atmospheric settings. The CNT loadings employed were targeted to include extremely low amounts of CNT (0.014 wt%) and a couple of compositions with low loadings (0.2 and 0.75 wt%). Such selection allowed the characterization of the behavior of specimens below and above electrical conductivity percolation limits, respectively, observed in prior work [50,51]. The resistivity of the CNT epoxy composites at 760 torr and 25 °C, is expected to be in the 2×10^3 to 10×10^3 Ohm-cm range for 0.014 wt% CNT, 50 to 200 Ohm-cm for 0.2 wt% CNT and 16 Ohm-cm or less for 0.75 wt% CNT. The standard

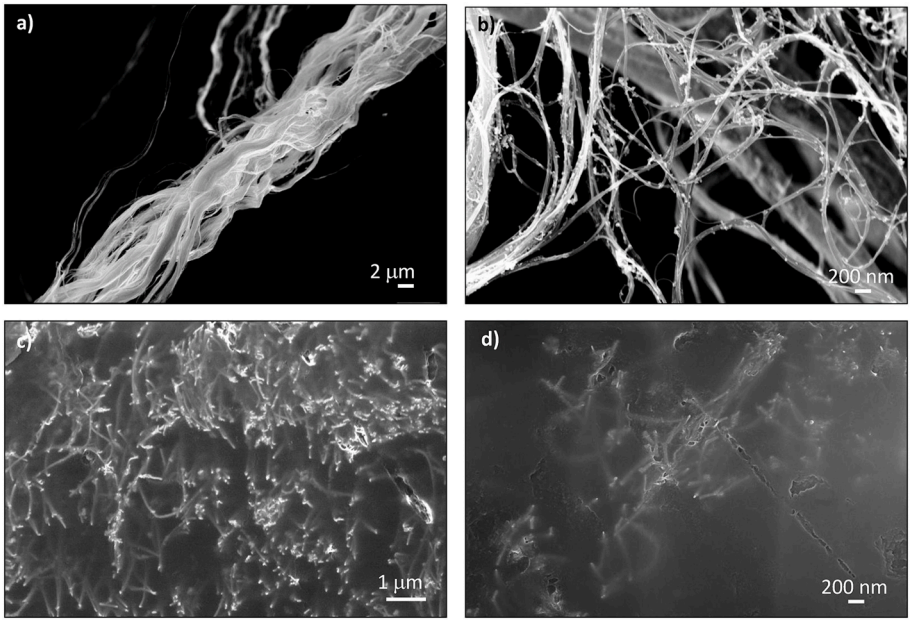

Fig. 6. a) and b) SEM micrographs of raw CNT bundles at different magnifications. c) and d) Distribution of CNT network within the epoxy composite for a specimen containing 0.75 wt% loading showing the conductive CNT tridimensional network alternated with void spaces.

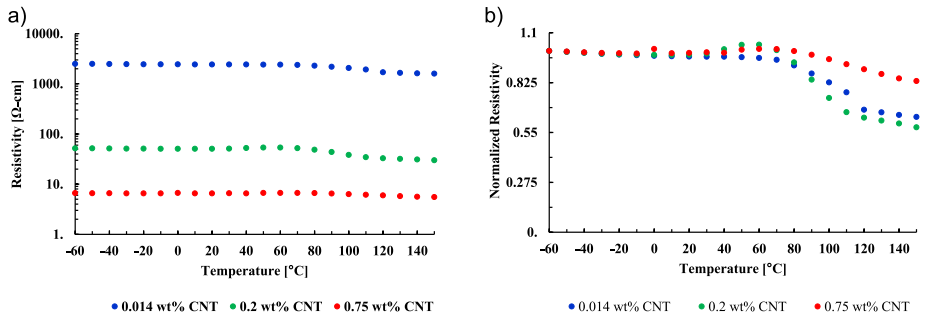

Fig. 7. Variation in resistivity recorded when samples are exposed to 1×10^{-6} torr and temperatures from −60 to 150 °C. a) Logarithmic scale and b) Normalized resistivity to compare the extent of the change by CNT loading.

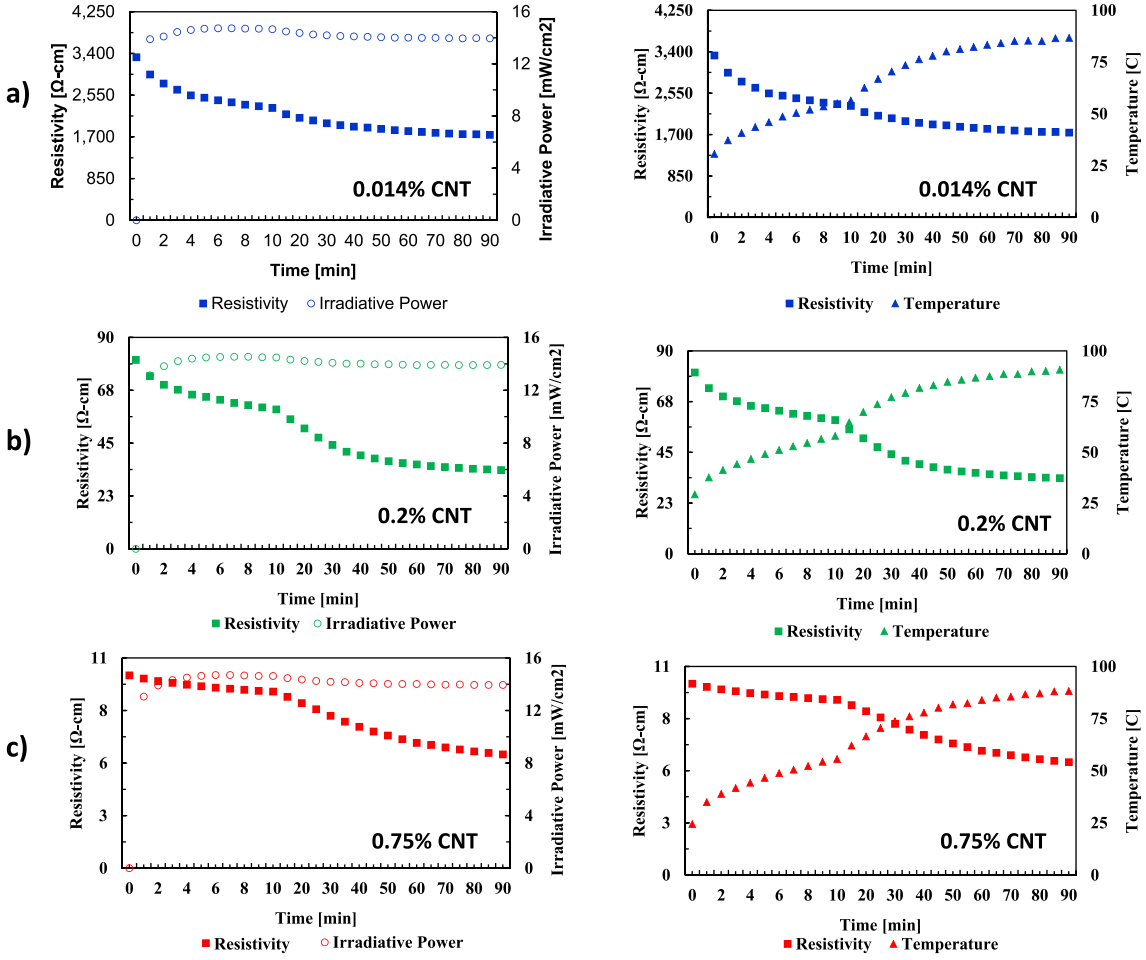

Fig. 8. Resistivity as a function of time of treatment as the samples are exposed to simulated sunlight for composites with a) 0.014, b) 0.2 and c) 0.75 wt% CNT loadings. Left: Including irradiance measured during exposure. Right: Including the increase in temperature generated as result of the sunlight exposure.

deviation in the data presented in the figure was calculated from the analysis of 8 different electric board samples. The resistivity range mentioned includes the lot-to-lot variability. Fig. 5 presents the electrical resistivity for composites with CNT loadings from 0.014 to 2 wt%. Some of the resistivity trends below 300 Ohm-cm could be appreciated in the inset graph. The SEM observation of the microstructural features for two compositions (0.014 and 0.75 CNT wt%), acquired from the epoxy-CNT composites polished surfaces, is presented as well, along a schematic representation of the conductive networks identified. For the SEM images, the bright areas correspond to the CNT embedded bundles. In the accompanying pictogram, the grey areas represent the locations of the composite densely populated by CNT, where electrons are expected to have high mobilities, while the blue regions represent insulating areas, where the epoxy is devoid of CNT. It is worth noting that the scale bar for each image is quite different: 10 μm for the 0.014 CNT wt% sample and 1 μm for the 0.75 CNT % specimen. The striking differences in resistivity as a function of filler loading are associated with the microstructural features: The absence of a conductive network in samples with 0.014 wt% CNT promotes a capacitor-like behavior. In contrast, the samples with 0.2 and 0.75 wt% CNT, despite containing regions devoid of CNT, form a tridimensional web of interconnected nanotube conductors within the non-conductive polymeric matrix, thus, exhibiting the expected resistor behavior. Detailed analysis of the conductive mechanisms in these composites, and some of the variables

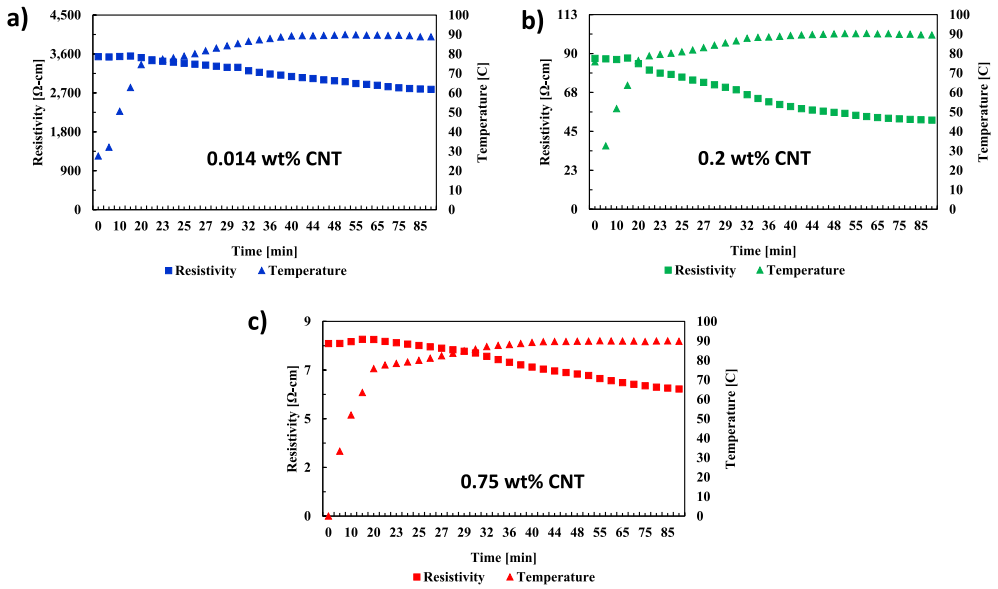

Fig. 9. Resistivity vs temperature for composites heating to 90 C in oven with a) 0.014, b) 0.2 and c) 0.75 wt% CNT loadings.

that influence them, can be found in Refs. [50,51].

Fig. 6 presents SEM micrographs in which bare CNT bundles could be appreciated (6a) and where the individual diameter and presence of Fe catalyst nanoparticles is evident (6b). Fig. 6c and d illustrate the microstructure of the 0.75 wt% CNT epoxy composite, showing the CNT distribution within the polymer at 10,000x and 20,000x, respectively. It is worth noting that these images show CNT at the surface of the composite as well as CNT strands that are embedded in the matrix, forming a connected network that extends in all directions. As previously mentioned, it is believed that the existence of such intertwined CNT web is responsible for the electrical conductivity of the composite.

3.2. TVAC environmental chamber

The resistivities observed as function of the low pressure and temperatures of the TVAC are presented in Fig. 7. The electrical behavior of the samples for the three loadings seemed practically unaffected at sub-ambient temperatures combined with low pressure. The graph presented in Fig. 7a shows an almost constant value of resistivity as the samples transition from −60 to 25 °C. The order of magnitude of the resistivity for each sample was within the expected values reported in Section 3.1. All the specimens exhibit a slight resistivity uptake followed by a significant reduction after the temperature surpasses 40 °C, with larger changes occurring between 70 and 110 °C and higher temperatures. Fig. 7b presents the normalized resistivity, assuming that the original reading for each filler loading is equal to 1. The samples with the lower loadings, 0.014 and 0.2 wt% CNT suffer the largest alteration, with reduction in resistivity of approximately 40% of their original values. The sample with 0.75 wt % displays only a reduction of 20%. Since most of the interest in these materials in space systems derives from their electrical conduction, the trends observed here are not expected to compromise their functionality but to improve their behavior.

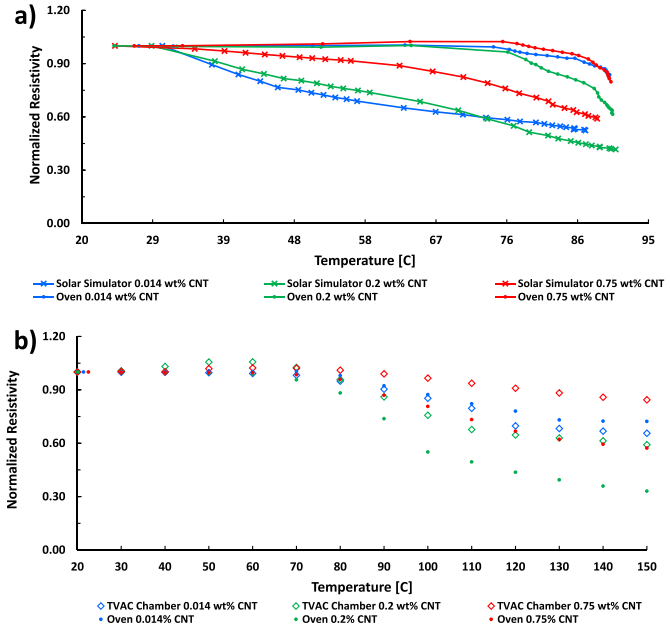

Fig. 10. Comparison of the effects that temperature caused by a) Simulated sunlight exposure vs convection oven and b) TVAC chamber vs convection oven, has in the composite specimens' resistivity.

As a parallel study, pristine composites were stored at sub-ambient pressures (114.76 Torr) in a Pelco 2251 vacuum desiccator chamber (Ted Pella Inc. Redding, CA, USA) and their resistivities recorded over time. Resistivity reductions were negligible for the first day, however, the effect of the low pressure becomes more evident with time, reaching reductions of 0.20, 24.6 and 5.67 % for the 0.014, 0.2 and 0.75 wt% CNT composites, respectively, after 20 days. Such results demonstrate that not only high vacuum, but simple sub-ambient pressures, are enough to produce a change in properties and serves as evidence that loss of moisture and other absorbed gases or volatile components from the epoxy resin might be occurring. The differences between the desiccator and TVAC indicate that outgassing of moisture absorbed by the CNT and/or the epoxy matrix could occur to a small extent under pressures below atmospheric and be exacerbated as the temperature increases or pressure decreases. Section 4 below includes the thermogravimetric analysis and further discusses the root cause of the electrical properties' fluctuations detected.

3.3. Solar simulator

The exposure of the samples to light produced by the solar simulator showed similar electrical behavior tendencies than the one observed for the TVAC experiment; an overall reduction in resistivity is observed as the time of exposure and temperature increased. The magnitude of the changes in resistivity in this case, is quite significant, with reductions of

48, 58 and 41% for the samples with 0.014, 0.2 and 0.75 wt% CNT, respectively. It is worth noting that the temperature of the samples increases asymptotically over time once the irradiance stabilizes as illustrated in Fig. 8.

In addition to the temperature effects, these samples experienced the exposure to electromagnetic radiation, which is known to produce an increase in the number of charge carriers, with the associated decrease in resistivity. The observed changes in the resistivity of the composites during their exposure to radiation in the UV, visible light and IR ranges, does not seem to follow a trend with respect to the CNT loading. The samples seem to be more susceptible to the level of porosity and surface characteristics than to loading, as the mass loss analysis presented in Section 4.1 will further address.

3.4. Convection oven

As previously mentioned, the experiments in the convection oven were meant to isolate the effect that temperature, as a single variable, had in the composite material's electrical properties. The curves generated are presented in Fig. 9. The resistivity of the samples seems to stay at the original value until the samples reach approximately 70 °C. After that, the temperature tends to increase logarithmically while the resistivity experiences exponential decay. It is worth noting that a small reduction of resistivity is still observed after the samples reach the maximum temperature. The specimens undergo a resistivity reduction of 21.4, 40.87 and 26.3% for samples with 0.014, 0.2 and 0.75 wt% CNT loadings, respectively. Thus, the oven samples suffered modest changes when compared to those seen for irradiance exposure over time in the solar simulator. In contrast, the electrical properties recorded in the oven from room temperature to 150° C at atmospheric pressure, are similar to those experienced in the TVAC under high vacuum and up to 150° C. Only the oven sample with 0.2 wt% CNT shows a more dramatic change. The mechanisms suspected of affecting composite resistivity are further discussed in the next section.

4. Discussion

4.1. Electrical properties measured in-situ

Fig. 10 presents a comparison of the magnitude of the changes in the composites resistivity for each setting described. The data has been normalized, for all loadings studied, to the resistivity value at starting temperature for a) oven and solar simulator and b) TVAC chamber. It is worth noting that each graph contains convection oven data and that each experiment used a different heating rate to mimic, to the extent possible, the conditions imposed by the solar simulator or the TVAC. When the effects of temperature in oven are contrasted with those of the combined temperature and exposure to simulated sunlight in Fig. 10a, it becomes evident that the combined irradiance and concomitant surge in temperature have the greater influence in the instantaneous changes in resistivity than temperature by itself. For TVAC (Fig. 10b), low temperatures (−60 to 25° C) and low pressures (up to 1×10^{-7} Torr) did not seem to modify the electrical performance (see Fig. 7), only higher temperatures result in significant resistivity reductions, thus the data here is only compared from 25 to 150 °C. From Fig. 10b, the oven experiment rendered a larger change in the resistivity than the TVAC. The location of the thermocouples in each experiment might provide a possible explanation; In the convection oven, the composite, and the overall volume of air inside the oven is at the setpoint temperature, while in the TVAC it is only the platen what is being heated. That is, the temperature imposed by the TVAC has to travel from the platen that acts as substrate, to the electric board (with thermally insulating backing) and finally to the composite. Thus, it is believed that in the oven the samples actually experience a more consistent heating process, which might produce higher localized temperatures, exacerbating its effects. Another observation from Fig. 10a and b, is that the 0.2% sample exhibits larger variation than other loadings under all conditions.

In all cases, the in-situ changes measured showed a significant decrease in the samples resistivity (increased conductivity), a factor that should be acknowledged as systems containing these composites are exposed to LEO conditions.

Several factors have been shown to impact electrical conduction in CNT composites at elevated temperatures. These include temperature dependent properties of the composite matrix material, differences in thermal expansion of components making up the matrix, thermal activation of charge carriers at elevated temperatures/thermal fluctuation induced tunneling, and interactions with the atmosphere [52,53]. The data collected and presented here seems to follow a similar tendency as those studies and puts in evidence that the property changes result from the instantaneous exposure and continue over time. Thermal induced tunneling proposed by Sanli et al. [54] and Sheng et al. [55], could apply to samples above percolation limit (0.2 and 0.75 wt% CNT in this work), however, it won't be responsible for the temperature effects seen in the 0.014 wt% CNT sample, where the separation between CNT strands is in the micrometer range. The exposure to light might have an independent effect since the overall magnitude of the changes in the solar simulator seem to be greater than those observed at the same or even greater temperatures in the TVAC or in the oven experiments. Light effects in semiconductors are similar to heat effects. In both cases, free electrons are generated with the concurrent reduction in resistivity. Reducing the pressure or increasing temperature seem to also produce outgassing. The analyses of the samples by thermogravimetry confirms that the application of temperature is accompanied by a reduction in mass as shown in Fig. 11. The 0.014, 0.2 and 0.75 wt% CNT epoxy composites show 2.51, 5.23 and 3.01% mass reduction, respectively. The bare epoxy (no CNT), Aero 9396 Loctite, recommended for space applications due to low off gassing, showed a mass loss of only 1.26%. The bare CNT pulp employed, containing still the Fe catalyst, showed a mass loss of 4.56%.

To understand why the sample with 0.2 wt% CNT lost more weight, the surface characteristics of all the composites were studied under an optical microscope. Despite all samples being produced under similar conditions, the sample with 0.2 wt% CNT presents a large amount of surface pores (Fig. 11b), not only are those of much larger dimensions (up to 100 μm) than the ones observed in the other two samples (Fig. 11a and c), their number far exceeds that of the other samples. The larger surface area produced by the porous surface could explain a greater tendency to absorb moisture that is lost during the heating cycles. In the images presented in Fig. 11 exemplary pores are marked with blue arrows. The white arrows in the sample that contains 0.75 wt % CNT

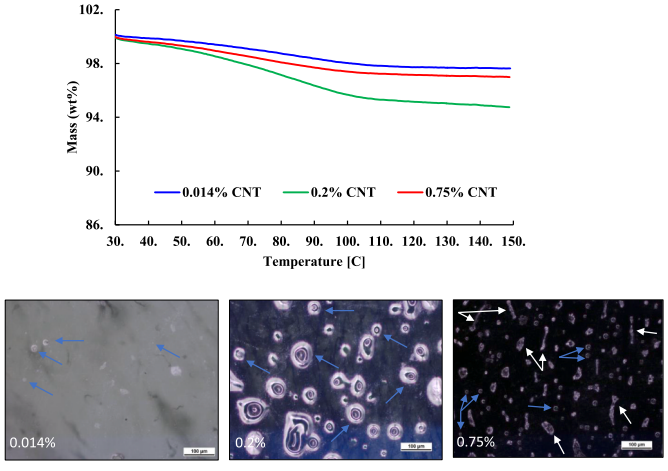

Fig. 11. Top: Mass loss recorded when conducting a thermogravimetric analysis of the composite samples over the range of temperatures of interest. Bottom: Optical microscopy images of the samples surface showing the presence of pores. Note: Scale in images 100 μm.

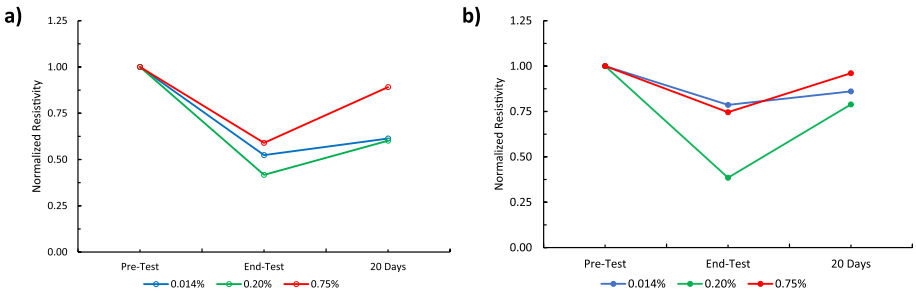

Fig. 12. a) Resistivity values pre- and post solar simulator exposure. b) Resistivity values pre-and post convection oven experiment.

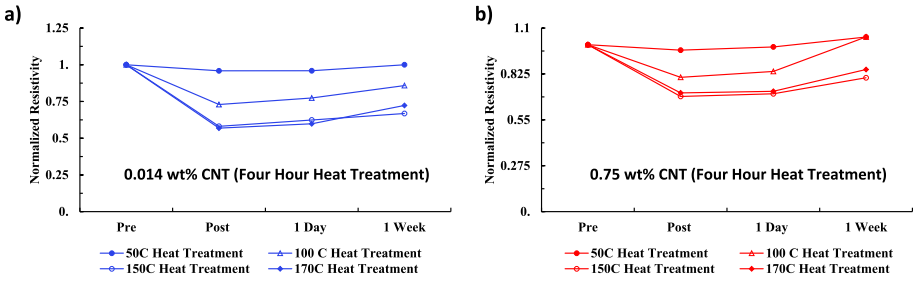

Fig. 13. Pre- and post heat treatment resistivity values for a) 0.014 and b) 0.75 wt% CNT.

represent areas of the sample where CNT are located at the surface, thus, creating a similar contrast than the ones that the spherical pores has. The shape of pores is in all cases a regular sphere, while the CNTs are shown as strings or irregular shapes.

Differences in the composite fabrication process, such as the level of applied vacuum prior to curing, possible air inclusion during addition of hardener, and time employed to create the conductive film could result in microstructural differences of the resulting epoxy. Larger loading percentages are prone to porosity issues due to the increased mixture viscosity and are especially susceptible to slight differences in preparation technique. Density differences of as much as 4.1% have been found for the same loadings due to differences in preparation procedures and could account for the differences seen via thermogravimetric analysis and optical microscopy.

4.2. *Electrical properties measured after exposing specimens back to atmospheric conditions*

Since the current study focused on the *instantaneous* electrical behavior of CNT epoxy composites during their exposure to LEO approximate temperatures, pressures and sunlight, no data is presented in regard to their behavior after prolonged periods of exposure. However, there was still interest on what the immediate changes will be if the composites were returned back to atmospheric conditions. The samples were stored in polyethylene vials at room temperature and pressure and their resistivity measured on the days following removal from the test environment. Fig. 12 presents the data collected before, after, and 20 days following temperature and UV testing.

As described in detail in previous sections, a resistivity decrease (conductivity increase) is observed for all the environments studied for all the CNT loadings. The resistivity after one day back to atmospheric conditions tends to remain at the same decreased values or suffer a minor increase. Mohiuddin et al. also noted lower resistance values in samples that were previously been subject to high temperatures, as reported in their study of the electrical resistance with increasing temperature for CNT-polyether ether ketone composites with CNT loadings between 8 and 10 wt% [56]. In the present study, after one week of the original experiments, the resistivity is greater but not quite back at the values recorded before the experiments under simulated environments were conducted. The result is significant since it shows that the species that originally outgassed from the samples, could be easily re-absorbed after a few days and that the temperature effects are, until a certain extent, reversible.

Such upturn in resistivity was also confirmed by heating pristine samples in the convection oven at a set temperature for 4 h and exposing them back to the laboratory atmosphere (see Fig. 13). The figure illustrates how the magnitude of resistivity reductions are proportional to the heating temperature for the same time of treatment. Those heated only to 50 °C had modest changes, while the samples heated at higher temperatures present a more significant relative change. Both the 0.014 and 0.75 wt% CNT samples showed resistivity values trending back to their original state after one week in atmospheric conditions. When comparing the trends between Figs. 12 and 13, it is clear that the samples that were simply heated using the oven returned to the original values much faster than those that were also exposed to sunlight.

It is expected that if the systems that contain these composites are exposed back to atmospheric conditions, as is the case in the reuse of some of the systems, their electrical properties will experience some level of recovery, as seen herein. A possible explanation of why the original values were not completely reached, might be that not all the volatiles initially lost are present in the atmosphere, some might be associated with the polymeric matrix components and thus, can't be reabsorbed by the sample surface. Moreover, the composite surface finishing will also have an impact on the extent of the changes observed.

5. Conclusions

The instantaneous changes in electrical properties of CNT epoxy composites containing low CNT loadings (less than 1%) were measured while the specimens were exposed to diverse simulated space conditions. A thermal vacuum chamber, solar simulator, and a convection oven were employed to produce approximate pressures, temperatures, and light conditions associated with low earth orbit. Increasing temperature above 60° C under high vacuum will produce an instant reduction in resistivity of at least 20%. Exposure to simulated sunlight can have major impacts in the electrical behavior, promoting a surge in temperature and causing resistivity reduction up to almost 60% of the original values. All observations are consistent with mass loss due to

volatile species outgassing, and the generation of extra charge carriers as result of UV/visible/IR light exposure. Surface porosity plays a critical role in the specimen's resistivity under all conditions studied. The latter seems to be more impactful than loading values when the CNT content is less than 1%. To a large extent, the changes in electrical properties observed were reversed after the specimens were returned to atmospheric conditions.

Credit author statement

Conceptualization conducted by Claudia Luhrs and Brian Earp, Data curation performed by Alexander Tracy, Brian Earp, Joel Hubbard, Dan Sakoda and Claudia Luhrs, Formal analysis done by Brian Earp, Joel Hubbard and Claudia Luhrs. Methodology Brian Earp, Joel Hubbard, Dan Sakoda. Project administration, Supervision and resources Claudia Luhrs. Validation Brian Earp, Joel Hubbard Writing - original draft Claudia Luhrs, Brian Earp, Joel Hubbard, Dan Sakoda. Writing - review and editing Joel Hubbard, Brian Earp, Claudia Luhrs.

Declaration of competing interest

The authors declare that they have no known competing financial interests or personal relationships that could have appeared to influence the work reported in this paper. The views expressed in this document are those of the author and do not reflect the official policy or position of the Department of Defense or the U.S. Government.

Acknowledgements

We thank Dr. Mohan Bahn, from OAI Instruments, for providing the solar simulator's spectral data presented in Fig. 2. Our team appreciates the support that Mr. David Rigmaiden provided by handling the LN2 dosing during the TVAC experiments.

References

[1] Khan W, Sharma R, Saini P. Carbon nanotube-based polymer composites: synthesis, properties and applications. In: Berber M, Hafez IH, editors. Carbon nanotub. - curr. Prog. Their polym. Compos. London, United Kingdom: Intech Open; 2016. p. 1–45. https://doi.org/10.5772/62497.

[2] Harris PJF. Carbon nanotube composites. Int Mater Rev 2004;49:31–43. https://doi.org/10.1179/095066004225010505.

[3] Backes EH, Sene TS, Passador FR, Pessan LA. Electrical, thermal and mechanical properties of epoxy/CNT/calcium carbonate nanocomposites. Mater Res 2018;21. https://doi.org/10.1590/1980-5373-mr-2017-0801.

[4] Yang C-K, Lee Y-R, Hsieh T-H, Chen T-H, Cheng T-C. Mechanical property of multiwall carbon nanotube reinforced polymer composites. Polym Polym Compos 2018;26:99–104. https://doi.org/10.1177/096739111802600112.

[5] Kausar A, Rafique I, Muhammad B. A review on applications of polymer/carbon nanotube and epoxy/CNT composites. Polym Plast Technol Eng 2016;55. https://doi.org/10.1080/03602559.2016.1163588.

[6] De Volder MFL, Tawfick SH, Baughman RH, Hart AJ. Carbon nanotubes: present and future commercial applications. Science 2013;339:535–9. https://doi.org/10.1126/science.1222453.

[7] Watson KA, Connell JW. Chapter 19 - polymer and carbon nanotube composites for space applications. In: Dai L, editor. Carbon nanotechnol. Amsterdam: Elsevier; 2006. p. 677–98. https://doi.org/10.1016/B978-044451855-2/50022-X.

[8] Bellucci S, Balasubramanian C, Micciulla F, Rinaldi G. CNT composites for aerospace applications. J Exp Nanosci 2007;2:193–206. https://doi.org/10.1080/17458080701376348.

[9] Udupa G, Rao SS, Gangadharan KV. Future applications of carbon nanotube reinforced functionally graded composite materials. In: IEEE-int conf adv eng sci manag ICAESM -2012; 2012. p. 399–404.

[10] Yadav R, Tirumali M, Wang X, Naebe M, Kandasubramanian B. Polymer composite for antistatic application in aerospace. Def Technol 2020;16:107–18. https://doi.org/10.1016/j.dt.2019.04.008.

[11] Smith J, Connell JW, Delozier DM, Lillehei P, Watson KA, Lin Y, et al. Space durable polymer/carbon nanotube films for electrostatic charge mitigation. Polymer 2004;45:825–36. https://doi.org/10.1016/j.polymer.2003.11.024.

[12] Samareh JA, Siochi EJ. Systems analysis of carbon nanotubes: opportunities and challenges for space applications. Nanotechnology 2017;28:372001. https://doi.org/10.1088/1361-6528/aa7c5a.

[13] Du J-H, Bai J, Cheng H-M. The present status and key problems of carbon nanotube based polymer composites. Express Polym Lett 2007;1:253–73. https://doi.org/10.3144/expresspolymlett.2007.39.

[14] Gojny FH, Wichmann MHG, Köpke U, Fiedler B, Schulte K. Carbon nanotube-reinforced epoxy-composites: enhanced stiffness and fracture toughness at low nanotube content. Compos Sci Technol 2004;15:2363–71. https://doi.org/10.1016/j.compscitech.2004.04.002.

[15] Yokozeki T, Iwahori Y, Ishibashi M, Yanagisawa T, Imai K, Arai M, et al. Fracture toughness improvement of CFRP laminates by dispersion of cup-stacked carbon nanotubes. Compos Sci Technol 2009;69:2268–73. https://doi.org/10.1016/j.compscitech.2008.12.017.

[16] Zhang X-H, Zhang Z-H, Xu W-J, Chen F-C, Deng J-R, Deng X. Toughening of cycloaliphatic epoxy resin by multiwalled carbon nanotubes. J Appl Polym Sci 2008;110:1351–7. https://doi.org/10.1002/app.28590.

[17] Zhang W, Picu RC, Koratkar N. Suppression of fatigue crack growth in carbon nanotube composites. Appl Phys Lett 2007;91:193109. https://doi.org/10.1063/1.2809457.

[18] Jen Y-M, Yang Y-H. A study of two-stage cumulative fatigue behavior for CNT/epoxy composites. Procedia Eng 2010;2.

[19] Jen Y-M, Wang Y-C. Stress concentration effect on the fatigue properties of carbon nanotube/epoxy composites. Compos B Eng 2012;43:1687–94. https://doi.org/10.1016/j.compositesb.2012.01.036.

[20] Loos MR, Yang J, Feke DL, Manas-Zloczower I. Enhanced fatigue life of carbon nanotube-reinforced epoxy composites. Polym Eng Sci 2012;52. https://doi.org/10.1002/pen.23145. 1882–7.

[21] Deng L, Young RJ, Kinloch IA, Sun R, Zhang G, Noé L, et al. Coefficient of thermal expansion of carbon nanotubes measured by Raman spectroscopy. Appl Phys Lett 2014;104:051907. https://doi.org/10.1063/1.4864056.

[22] Kumar P, Maiti UN, Sikdar A, Das TK, Kumar A, Sudarsan V. Recent advances in polymer and polymer composites for electromagnetic interference shielding: review and future prospects. Polym Rev 2019;59:687–738. https://doi.org/10.1080/15583724.2019.1625058.

[23] Sampaio J, Wnuk E, Vilhena de Moraes R, Fernandes S. Resonant orbital dynamics in LEO region: space debris in focus. Math Probl Eng 2014;2014:1–12. https://doi.org/10.1155/2014/929810.

[24] LEO. Parameters n.d. http://www.spaceacademy.net.au/watch/track/leopars.htm. accessed November 22, 2020.

[25] Iridium Satellite Communications | Truly Global Communications. Iridium satell commun n.d. https://www.iridium.com/. accessed November 24, 2020.

[26] SpaceX submits paperwork for 30,000 more Starlink satellites - SpaceNews n.d. https://spacenews.com/spacex-submits-paperwork-for-30000-more-starlink-satellites/(accessed November 24, 2020).

[27] Colton K, Breu J, Klofas B, Marler S, Norgan C, Waldram M. Merging diverse architecture for multi-mission support. Small Satell Conf 2020. https://digitalcommons.usu.edu/smallsat/2020/all2020/158/.

[28] Micheli D, Apollo C, Pastore R, Bueno Morles R, Coluzzi P, Marchetti M. Temperature, atomic oxygen and outgassing effects on dielectric parameters and electrical properties of nanostructured composite carbon-based materials. Acta Astronaut 2012;76:127–35. https://doi.org/10.1016/j.actaastro.2012.02.019.

[29] Tucci V, Guadagno L, Raimondo M, Vittoria V, Vertuccio L, Naddeo C, et al. Development of epoxy mixtures for application in aeronautics and aerospace. RSC Adv 2014;4. https://doi.org/10.1039/C3RA48031C.

[30] Samwel S. Low earth orbital atomic oxygen erosion effect on spacecraft materials. Space Res J 2014;7:1–13. https://doi.org/10.3923/srj.2014.1.13.

[31] ARES. Orbital debris program office. Q Newsl 2009;13.

[32] NASA. Technical reports server (NTRS) n.d. https://ntrs.nasa.gov/citations/20030062195. accessed November 22, 2020.

[33] Hopkins AR, Labatete-Goeppinger AC, Kim H, Katzman HA. Space survivability of carbon nanotube yarn material in low Earth orbit. Carbon 2016;107:77–86. https://doi.org/10.1016/j.carbon.2016.05.040.

[34] Ishikawa Y, Fuchita Y, Hitomi T, Inoue Y, Karita M, Hayashi K, et al. Survivability of carbon nanotubes in space. Acta Astronaut 2019;165:129–38. https://doi.org/10.1016/j.actaastro.2019.07.024.

[35] Kemnitz RA, Cobb GR, Singh AK, Hartsfield CR. Characterization of simulated low earth orbit space environment effects on acid-spun carbon nanotube yarns. Mater Des 2019;184:108178. https://doi.org/10.1016/j.matdes.2019.108178.

[36] Cobb GR, O'Hara RP, Kemnitz RA, Sabelkin VP, Doane BM. Quantifying the effects of ultraviolet type C radiation on the mechanical and electrical properties of carbon nanotube sheet for space-based applications. Mater Today Commun 2019;18:7–13. https://doi.org/10.1016/j.mtcomm.2018.10.016.

[37] Jiao L, Gu Y, Wang S, Yang Z, Wang H, Li Q, et al. Atomic oxygen exposure behaviors of CVD-grown carbon nanotube film and its polymer composite film. Compos Part Appl Sci Manuf 2015;71:116–25. https://doi.org/10.1016/j.compositesa.2015.01.008.

[38] Prusty RK, Rathore DK, Ray BC. CNT/polymer interface in polymeric composites and its sensitivity study at different environments. Adv Colloid Interface Sci 2017;240:77–106. https://doi.org/10.1016/j.cis.2016.12.008.

[39] Han J-H, Kim C-G. Low earth orbit space environment simulation and its effects on graphite/epoxy composites. Compos Struct 2006;72:218–26. https://doi.org/10.1016/j.compstruct.2004.11.007.

[40] Awaja F, Moon JB, Gilbert M, Zhang S, Kim CG, Pigram PJ. Surface molecular degradation of selected high performance polymer composites under low earth orbit environmental conditions. Polym Degrad Stabil 2011;96:1301–9. https://doi.org/10.1016/j.polymdegradstab.2011.04.001.

[41] Atar N, Grossman E, Gouzman I, Bolker A, Murray VJ, Marshall BC, et al. Atomic-oxygen-durable and electrically-conductive CNT-POSS-polyimide flexible films for space applications. ACS Appl Mater Interfaces 2015;7:12047–56. https://doi.org/10.1021/acsami.5b02200.

[42] Garcia M. Space debris and human spacecraft. NASA 2015. http://www.nasa.gov/mission_pages/station/news/orbital_debris.html. accessed November 22, 2020.
[43] Earp B, Dunn D, Phillips J, Agrawal R, Ansell T, Aceves P, et al. Enhancement of electrical conductivity of carbon nanotube sheets through copper addition using reduction expansion synthesis. Mater Res Bull 2020;131:110969. https://doi.org/10.1016/j.materresbull.2020.110969.
[44] Technologies N. Nanocomp technologies' products | sheet/tape n.d. https://www.miralon.com/sheet/tape. accessed March 25, 2021.
[45] LOCTITE. EA 9396 AERO n.d. https://www.henkel-adhesives.com/vn/en/product/adhesives/loctite_ea_9396_aero.html. accessed January 28, 2021.
[46] altitude_press_conv_table_low.pdf n.d.
[47] E21 Committee. Standard solar constant and zero air mass solar spectral irradiance tables. ASTM International; n.d. https://doi.org/10.1520/E0490-00AR19.
[48] Gueymard CA. The sun's total and spectral irradiance for solar energy applications and solar radiation models. Sol Energy 2004;76:423–53. https://doi.org/10.1016/j.solener.2003.08.039.
[49] Ustun TS, Nakamura Y, Hashimoto J, Otani K. Performance analysis of PV panels based on different technologies after two years of outdoor exposure in Fukushima, Japan. Renew Energy 2018;136. https://doi.org/10.1016/j.renene.2018.12.100.
[50] Earp B, Phillips J, Grbovic D, Vidmar S, Porter M, Luhrs CC. Impact of current and temperature on extremely low loading epoxy-CNT conductive composites. Polymers 2020;12:867. https://doi.org/10.3390/polym12040867.
[51] Earp B, Simpson J, Phillips J, Grbovic D, Vidmar S, McCarthy J, et al. Electrically conductive CNT composites at loadings below theoretical percolation values. Nanomaterials 2019;9:491. https://doi.org/10.3390/nano9040491.
[52] Shen JT, Buschhorn ST, De Hosson JThM, Schulte K, Fiedler B. Pressure and temperature induced electrical resistance change in nano-carbon/epoxy composites. Compos Sci Technol 2015;115:1–8. https://doi.org/10.1016/j.compscitech.2015.04.016.
[53] Li Q, Xue QZ, Gao XL, Zheng QB. Temperature dependence of the electrical properties of the carbon nanotube/polymer composites. Express Polym Lett 2009;3:769–77. https://doi.org/10.3144/expresspolymlett.2009.95.
[54] Sanli A. Investigation of temperature effect on the electrical properties of MWCNTs/epoxy nanocomposites by electrochemical impedance spectroscopy. Adv Compos Mater 2019. https://doi.org/10.1080/09243046.2019.1616409.
[55] SHENG P. Fluctuation-induced tunneling conduction in disordered materials. Phys Rev B 1980;21:2180–95. https://doi.org/10.1103/PhysRevB.21.2180.
[56] Mohiuddin M, Van Hoa S. Electrical resistance of CNT-PEEK composites under compression at different temperatures. Nanoscale Res Lett 2011;6. https://doi.org/10.1186/1556-276X-6-419.